

# Design of a Rehabilitation Exoskeleton with Impedance Control: First Experiments

Gaëtan Courtois<sup>1</sup>, Jason Chevrier<sup>1</sup>, Antoine Dequidt<sup>1,2</sup>, Xavier Bonnet<sup>3</sup> and Philippe Pudlo<sup>1</sup>

<sup>1</sup>Univ. Polytechnique Hauts-de-France, LAMIH, CNRS, UMR 8201, F-59313 Valenciennes, France

<sup>2</sup>INSA Hauts-de-France, F-59313 Valenciennes, France

<sup>3</sup>Institut de Biomécanique Humaine Georges Charpak, Arts et Métiers Paristech, 151 Boulevard de l'Hôpital, F-75013 Paris, France

**Keywords:** Lower-Limb Exoskeleton, Impedance Control, Gait Rehabilitation.

**Abstract:** In this paper, we disclose the design strategy, control design and preliminary works leading to the development of a post stroke gait rehabilitation exoskeleton. The strategy is established based on the conventional gait rehabilitation currently used in rehabilitation centers and defines the exoskeleton as an interface between the therapist and the patient. The final purpose of this interface is to complete the conventional rehabilitation by intensifying the work of the patient while relieving the physical burden on the therapist. As the conventional rehabilitation is based on successive exercises the control is designed to have several operating modes triggered depending on the currently processing exercise. A test bench was realised to evaluate quantitatively as well as qualitatively these operating modes. Preliminary results of quantitative experiments on the transparent operation mode are then presented. These results validate the control design and comfort us on our development method.

## 1 INTRODUCTION

Today the most important cause of hemiplegia is cerebrovascular accident or stroke. Each year around 13.7 million cases are counted in the world (Feigin et al., 2019). Only 85% of the survivors of a stroke can walk after 6 months. Among them 5% are said to be severe hemiplegics and don't regain their full autonomy (Olney et al., 1996). Then around 20% of the survivors of a stroke never recover even if some of them followed a rehabilitation therapy.

In this context of ever-increasing number of people suffering from hemiplegia, due to a lack of manpower rehabilitation centers are forced to select the accepted patients. Hence a lot of people cannot follow a gait rehabilitation therapy and eventually lose their autonomy.

One of the solutions to help the therapists to accept more patients is to propose tools like exoskeletons to increase the chances of rehabilitation of post stroke patients, even for the most severe cases.

Nowadays there are numerous lower-limb exoskeletons which are used or studied for the rehabilitation. And even among only the

anthropomorphic ones it is still possible to find a lot of exoskeletons used for rehabilitation (Denis et al., 2016 and Esquenazi et al., 2017). However, this kind of exoskeletons is not proven to improve the gait rehabilitation compared to conventional rehabilitation (Pennycott et al., 2012). Furthermore, to the best of our knowledge none of them was designed specifically for post stroke gait rehabilitation. This way the final aim of this work is to design an exoskeleton specifically thought for the gait rehabilitation of hemiplegic patients.

During conventional rehabilitation post stroke patients pass through different stages, namely passive, semi-active and active patient. Each can be seen as a functioning mode of the developed exoskeleton.

Impedance control is very well-suited for the interaction between patient and exoskeleton and is really adaptable to these 3 phases of the rehabilitation. Hence, in this context, impedance control is the most appropriate for gait rehabilitation (Akdoğan et al., 2018). Moreover, one of the most important operating modes of rehabilitation exoskeletons is the transparent mode (Andrade et al., 2019) and impedance control is one of the most suitable to achieve transparency (Tucker et al. 2015).

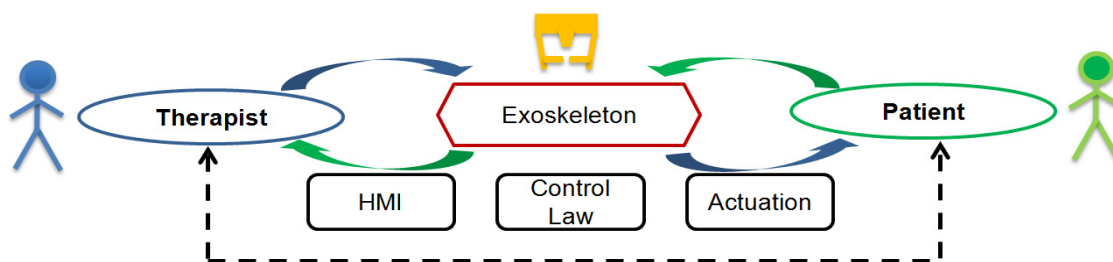


Figure 1: Schematic representation of the rehabilitation strategy.

In this context this paper focuses on the preliminary works on transparency made to develop the first prototype of this exoskeleton designed for post stroke gait rehabilitation. Section 2 displays the elements leading to the design of a hip only actuated exoskeleton. Section 3 details the formulation of an hybrid impedance control law and how it applies to transparent operation mode. Section 4 describes the preliminary experiments on transparency made on a test bench and shows the results. Finally, Section 5 concludes this paper and opens the way for further developments.

## 2 DESIGN OF A HIP ACTUATED EXOSKELETON

The first prototype we developed is a hip only actuated exoskeleton. According to the therapists the hip is indeed the most important joint to start the rehabilitation. However, to understand the design of this first prototype the first thing to explain is the rehabilitation strategy.

### 2.1 Rehabilitation Strategy

Rehabilitation is a domain which requires knowledge and know-how that only specialists can show. So, we choose to work with therapists to design the exoskeleton as a tool for the therapists made by the therapists.

In other words, for further developments the exoskeleton is described as an interface between the therapist and the patient as shown in Figure 1. Its purpose is to intensify the conventional rehabilitation and to allow sub-acute patients to access to the rehabilitation platforms.

#### 2.1.1 Therapist-exoskeleton Interface

The interaction between the therapist and the exoskeleton is made by a human-machine interface (HMI). This interface is designed with the therapists

to make full use of their know-how thanks to the several fonctionnalités available.

This HMI is designed to allow the therapist to plan a rehabilitation session following the pattern of the conventional rehabilitation. It means that the therapist will choose exercises for the patient to realise while assisted by the exoskeleton.

These exercises are designed by the therapists and then translated to write the control laws. Thus each exercise corresponds to a control with personalized parameters. Moreover, all these parameters can be adjusted in real time by the therapists via the HMI.

#### 2.1.2 Exoskeleton-patient Interface

Some choices were needed about the exoskeleton-patient interaction to design our gait rehabilitation exoskeleton. First, to lessen the power consumption needed to stabilise the patients and to sustain their weight our first choice was to use a body weight support.

Moreover, the gait pattern has been known for decades by the therapists and they also know that the hip can be actuated only in the sagittal plane for the gait rehabilitation. Then as shown in Figure 2, the design can be simplified to put only one actuator in this plane, which simplifies the control as well.



Figure 2: First prototype - Hip only actuated exoskeleton.

To sum up the exoskeleton's final version's purpose is to replace the hands of the therapist to improve the rehabilitation of the patient while maintaining the comfort of both of them.

## 2.2 Actuation Design

The actuation design regroups 3 important devices: the servodrive, the motor and the gear. First, the most important requirements are set as the weight and the bulkiness of the system that need to be as low as possible. Since the controller is used to compensate the mechanical impedance, it is not included in the design requirements. Thus, the servodrive should allow implementing custom control laws for this compensation. The controller (Embedded PC) and the servo drive must therefore be able to implement customized control laws for this compensation. The servodrive must then be configured in cyclic synchronous torque (CST) mode and the EtherCAT fieldbus, which is widely used in industry, is therefore particularly suitable for ensuring controller-servodrive communication with cycle times of less than 1 ms.

Moreover, to be freed from the problem of homologation, all the components were picked from supplier's catalogs to meet reliability and safety standards (ISO 13849-1, IEC 62061).

The last important requirement that drives the design is the torque needed for the gait rehabilitation. The average torque needed at the hip joint is around 1Nm normalized per patient weight (Giovacchini et al., 2014 and Seo et al., 2016). This way some of the already available exoskeletons can develop more than 100 Nm at the hip to fit a large population (Chen et al., 2019). However, due to the bodyweight support, it was fixed with the therapists that the max repeated torque needed can be reduced to around 40 Nm at the hip.

Eventually at the scale of a wearable exoskeleton, the most suitable device for the actuation is a brushless DC motor because of its power density (Manna et al. 2018). Then the three devices we have chosen are a servodrive EL7411 from Beckhoff company, a BLDC motor EC 90 Flat (+ Encoder MILE 2) from Maxon company and a CPU-17A from HarmonicDrive company with reduction ratio of 80:1. This actuation allows a max repeated torque of 43Nm for a weight of 1.55kg, which fulfills the requirement.

## 3 IMPEDANCE CONTROL FOR LOWER LIMB EXOSKELETON

The hybrid impedance control law used is based on the work of Akdogan et al. (2018). This control appears to be well suited for the purpose of exoskeleton assisted rehabilitation as it can be adapted to nearly every kind of environment (Anderson et al., 1987 and Akdogan et al., 2018). However, as this study is about the preliminary work of a hip only actuated exoskeleton, it is necessary to adapt the controller used by Akdogan et al. for 3 joints upper-limb actuation to a 1 joint lower-limb actuation.

### 3.1 System Dynamic Model

First, let us define the model used to describe the system dynamics as:

$$\tau = I\ddot{q} + F(q, \dot{q}) + G(q) - \tau_e, \quad (1)$$

where  $\tau$  is the gear output actuation torque,  $q$ ,  $\dot{q}$  and  $\ddot{q}$  are, respectively, the position, velocity and acceleration of the revolute joint,  $I$  is the inertia term,  $F(q, \dot{q})$  is the friction term,  $G(q)$  is the gravity term and  $\tau_e$  is the torque resulting from the force applied by the human limb.

### 3.2 Position-based Impedance Control Applied to Lower-limb Exoskeleton

One of the components of the hybrid impedance control law is the position-based impedance control. This controller is mostly used to help as needed when the patients are passive or when they don't have too much difficulties following the desired trajectory.

Then based on Akdogan et al. (2018) the desired dynamic behavior written in the exoskeleton joint space after applying the position-based impedance control can be given as:

$$I_d(\ddot{q} - \ddot{q}_d) + B_d(\dot{q} - \dot{q}_d) + K_d(q - q_d) = -\tau_e, \quad (2)$$

where  $I_d$ ,  $B_d$  and  $K_d$  are, respectively, the desired inertia, damping and stiffness at the joint and  $q_d$ ,  $\dot{q}_d$  and  $\ddot{q}_d$  are, respectively, the desired position, velocity and acceleration of the joint.

Still based on Akdogan et al. (2018) it is possible to rewrite the position-based impedance control as:

$$\tau = \frac{I}{I_d} [I_d \ddot{q}_d - B_d(\dot{q} - \dot{q}_d) - K_d(q - q_d)] - (1 + \frac{I}{I_d})\tau_e + \tau_c(q, \dot{q}) \quad (3)$$

where  $\tau_c(q, \dot{q})$  expresses the compensation terms depending on the system.

### 3.3 Force-based Impedance Control Applied to Lower-limb Exoskeleton

It can be said that the force-based control is more appropriate for the cases where the environment impedance is more important than the system impedance. As the patient represents the greater part of the exoskeleton environment the force-based impedance control becomes more suitable when the rehabilitation progresses (Tucker et al. 2015).

#### 3.3.1 Force-based Impedance Control for Semi-active Patient

When the patient becomes more active then the exoskeleton should be proportionally less active to favour the patient's progress.

Then the force-based impedance control gains in pertinence starting from the semi-active patient. This control allows managing the start of the exercises by perceiving the patient's intention and reacting accordingly (this issue is beyond the scope of this paper). Moreover, it can be used to help the patient when this one is not able to follow the trajectory by providing a greater torque allowing to complete the movement. In a rehabilitation context it is more important for the patient to finish the exercise than perfectly following the trajectory.

The desired dynamic behavior of the joint for the force-based impedance control inspired by Akdogan et al. (2018) can be written as follows:

$$I_d \ddot{q} + B_d \dot{q} - \tau_d = -\tau_e \quad (4)$$

where  $\tau_d$  is the desired torque applied on the limb. Then the force-based impedance control law can be written as follows:

$$\tau = \frac{I}{I_d} (\tau_d - B_d \dot{q}) - (1 + \frac{I}{I_d})\tau_e + \tau_c(q, \dot{q}) \quad (5)$$

#### 3.3.2 Transparent Operation Mode

Since impaired people are easier to hinder, it is then necessary to lessen everything that can be perceived as a burden for them (Andrade et al., 2019). The

transparency consists in minimizing the perception of the resistance of the system. Hence, it is the first operating mode that needs to be operational in case of rehabilitation.

In the case of post stroke gait rehabilitation, the transparency is mostly useful for two things. The first one is to let the patients move their unimpaired limb. Indeed, hemiplegia means that only one side of the body needs rehabilitation. Then as the patients are already weak from the stroke, the exoskeleton should not hinder their movements.

The second one is for patients near the end of the rehabilitation, who are more active. Then for the rehabilitation to pursue effectively, the exoskeleton should not assist nor hinder the patients during the exercises.

As these two cases are mostly for active or semi-active limbs the most appropriate control for the transparency is the force-based impedance control and the desired torque  $\tau_d$  is set to 0 for the patients to perceive no resistance. Hence (5) becomes:

$$\tau = -\frac{I}{I_d} B_d \dot{q} - (1 + \frac{I}{I_d})\tau_e + \tau_c(q, \dot{q}) \quad (6)$$

Finally, this transparent operation mode is the default mode. Otherwise, while not in transparent operation mode nor in an exercise the exoskeleton could be perceived as in a resistive mode. With transparency as the default mode, the exoskeleton can just assist as needed when it is needed.

### 3.4 Hybrid Impedance Control Applied to Lower-limb Exoskeleton

In the end, the hybrid impedance control is a combination of the previously presented control laws. Following the same pattern as in Section 3.2 and Section 3.3 the desired dynamic behavior resulting from the combination of (2) and (4) is as follows:

$$I_d(\ddot{q} - S\ddot{q}_d) + B_d(\dot{q} - S\dot{q}_d) + SK_d(q - q_d) + (1 - S)\tau_d = -\tau_e \quad (7)$$

where  $S$  can take the value 0 and 1 to switch between (4) and (2), respectively.

Hence the overall control law can be written as a combination of (3) and (5) as follows:

$$\tau = \frac{I}{I_d} (SI_d \ddot{q}_d - B_d(\dot{q} - S\dot{q}_d) - SK_d(q - q_d) + (1 - S)\tau_d) - (1 + \frac{I}{I_d})\tau_e + \tau_c(q, \dot{q}) \quad (8)$$

Roughly speaking, giving the value 0 or 1 to  $S$  allows switching the control in real time and thus adapting the comportment of the exoskeleton to assist the patients as needed. Moreover, the three parameters  $I_d$ ,  $B_d$  and  $K_d$  can also be modified according to the therapist's needs to adapt to each patient.

This versatility will be useful for the chosen rehabilitation strategy. Indeed, each exercise will depend of the patient rehabilitation state and this evolution of the patient also means an evolution of the environment's impedance.

## 4 EXPERIMENTS AND RESULTS

This section's purpose is to display the results of preliminary experiments. The first part is about the test bench and the identification of its model. Then the last two parts explain the first experiment about transparency and the first experiment with a simple position-based impedance control.

### 4.1 Test Bench

The test bench shown in Figure 3 is made using the same actuation system described in Section 2.2. Its purpose is to test this actuation system and the control law.

#### 4.1.1 Bench Description

This bench is designed to be used for qualitative experiments with the therapists as well as for quantitative experiments to validate the software and the devices.

For the qualitative tests the bench is designed to reproduce the kinematics of the hip exoskeleton according to the features mentioned in Section 2.1.2 and to be driven with a manual handle. The human hand being much more sensitive, it is expected that future experiments on transparency and on the

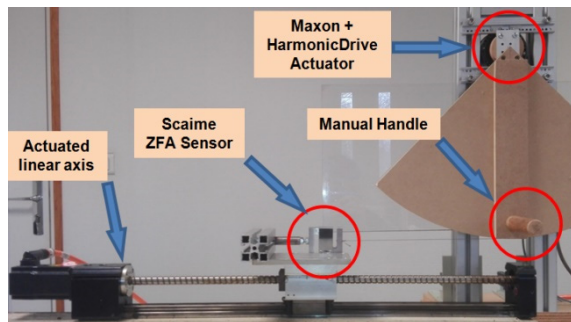


Figure 3: Test bench for preliminary experiments.

exercises will be more conclusive. This bench allows a wide range of tests to be carried out with several different users, including therapists.

For the quantitative experiments the bench is driven by a linear actuator controlled in position or velocity to ensure the reproducibility of the protocol. A cable wound up on a circular drum attached to the joint is connected to the linear actuator carriage. The tension force of the cable is measured by a monodimensional Scaime ZFA force sensor with a rated capacity of 25kg as shown in Figure 3. Knowing the radius of the drum, the measured force allows computing the torque  $\tau_e$  while the joint position and velocity are derived from the servodrive's processing of the motor's encoder signals.

#### 4.1.2 Identification of a Compensation Model

In order to implement the compensation term,  $\tau_c(q, \dot{q})$ , in the control law given in (8) an adequate representation of the system behavior should first be chosen and estimated. In this work, the test bench is assumed to follow the dynamic model given in (1). The friction term  $F(q, \dot{q})$  is chosen as a Coulomb-viscous model, the nonlinear term  $G(q)$  accounts for the effect of the gravity and the external torque  $\tau_e$  is set to zero, such that:

$$\tau = I \ddot{q} + F_v \dot{q} + F_c \text{sign}(\dot{q}) + C_g \sin(q), \quad (9)$$

where  $F_v$  and  $F_c$  are the viscous and dry friction coefficients, respectively,  $C_g$  is a gravity coefficient and  $I$  was defined in (1).

The values of the parameters for the test bench are identified from experimental measures using the DIDIM algorithm (Gautier et al., 2013). A 10 seconds periodic trajectory represented as a finite Fourier series is computed for optimal excitation of the parameters (Swevers et al., 1997) and 25 periods of this trajectory are applied to the system. Motor torque measures are acquired at a sample rate of 2 kHz and the average period is computed to reduce torque noise. The averaged samples are then filtered by a 10.66 Hz Chebyshev filter and decimated by a factor of 150 before being used as input for the DIDIM algorithm. Identified values of the parameters are given in Table 1.

The compensation term in (8) is then computed according to:

$$\tau_c(q, \dot{q}) = F_v \dot{q} + F_c \tanh\left(\frac{\dot{q}}{r}\right) + C_g \sin(q), \quad (10)$$

where the sign function in (9) is replaced by a hyperbolic tangent function for stability purposes, using a coefficient empirically tuned to  $r = 0.0375$ .

Table 1: Results of the DIDIM identification.

Parameter [unit]	Estimated value (relative standard deviation)
$C_g$ [N.m]	2.000 ( $\pm 6.06\%$ )
$F_v$ [N.m.s/ $^\circ$ ]	$5.584 \times 10^{-2}$ ( $\pm 5.26\%$ )
$F_c$ [N.m]	2.602 ( $\pm 2.21\%$ )
$I$ [kg.m $^2$ ]	2.042 ( $\pm 3.31\%$ )

## 4.2 Transparent Operation Mode: Preliminary Experiment

Knowing a model of the test bench, this section presents a first experiment to validate quantitatively the effect of the transparent operation mode. For this purpose, an experimental protocol was followed on the test bench.

### 4.2.1 Protocol

For the transparency, the control law is force-based as shown in (6). However, without a closed-loop in force  $\tau_e = 0$  and  $I_d$  is set to  $I$  and  $B_d$  to 0. The implemented control law thus becomes:

$$\tau = \tau_c(q, \dot{q}). \quad (11)$$

The experiment consists of 20 successive trajectories at constant velocities between 10 $^\circ$ /s and 30 $^\circ$ /s. This way a curve can be drawn to display the evolution of the torque depending on the velocity. Thus, the comparison between the curves with and without compensation can show the effect of the transparent operation mode.

### 4.2.2 Results

The results of this first experiment are displayed in Figure 4. The blue points are the average torque without compensation and the red ones represent the average torque with the compensation for the same velocity values.

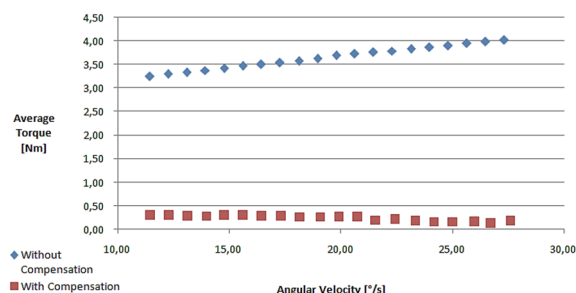


Figure 4: Comparison of the average torque needed for several velocities with and without compensation.

As anticipated the average torque measured with the compensation is quasi constant and very close to 0. These results show that this model can achieve transparency.

However, this diagram shows that the transparency can be improved. Even if the torque should not reach 0, for stability purposes, it seems possible to adjust the parameters to move closer to 0. Furthermore (6) is not fully exploited. Hence, these results are quite encouraging for further developments about the transparent operation mode.

## 4.3 Position-based Impedance Control: Preliminary Experiment

This second experiment is presented to test the identified compensation model while applying a position-based impedance control. The purpose of this experiment is to compare the behavior of the system with and without the compensation.

### 4.3.1 Protocol

In this experiment the control law (3) is used with  $I_d = I$ ,  $\ddot{q}_d = 0$ ,  $B_d = 0$  and without closed-loop in force so  $\tau_e = 0$ . This way it applies a constant stiffness mimicking a spring and can be written as follows:

$$\tau = -K_d(q - q_d) + \tau_c(q, \dot{q}), \quad (12)$$

where  $q_d = -45^\circ$  is the initial angular position of the handle and  $K_d = 0.3686 \text{ Nm}/^\circ$  is the stiffness of the virtual spring attached to  $q_0$ .

The experiment consists of 20 successive round trips of the linear actuator between  $-45^\circ$  and  $35^\circ$  of the handle. The velocity is maintained during all the successive experiments at a constant value of 20.25 $^\circ$ /s (seen at the handle). This way the measures allow the comparison of the system's response with and without the compensation.

### 4.3.2 Results

The results of this second experiment are shown in Figure 5. In green is displayed the theoretical value of the torque given by the virtual spring. The blue curve displays the torque of the average cycle without the compensation and the red one with the compensation.

First of all, the compensation shows clearly its effects during the going part. In this part of the cycle the compensation corresponds to the expectations based on the results in Section 4.2.2.

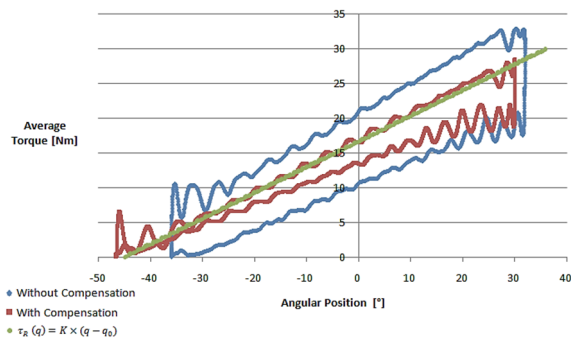


Figure 5: Comparison of the average torque with and without compensation while applying a compliance  $\tau_R(q)$ .

Two other details are also noticeable. The first one is the presence of the oscillations seen during the transient phases. (Knowing that  $B_d = 0$  this could be expected.) In practice, these disturbances are not desired for future applications. However, it should not be forgotten that the control law used in this preliminary experiment is not the full one as shown in (3) so the other terms, especially  $B_d$ , could be used to attenuate these oscillations.

The second and the most important issue on this diagram is the non symmetry of the red curve around the green one. This non symmetry shows the limit of our test bench which is quite usable for this preliminary experiment but lacks some precision in the metrology.

## 5 CONCLUSIONS

The developments to achieve the first prototype of this gait rehabilitation-oriented exoskeleton are near to the end and the results of the preliminary tests are encouraging. Currently the expectations were met even if the results showed some of the test bench limits.

For the next developments the first thing to do will be to optimise the test bench to be able to apply the full control law.

In a second time it is planned to implement a disturbance observer to estimate the interactive force between the patient and the exoskeleton. Therefore, it will be possible to analyze some robust control schemes with force closed loop.

These two points will allow us to implement the overall control law and test it quantitatively on the test bench. Furthermore, it will also be possible to qualitatively test it with the manual handle to improve the perception according to the therapists' feedback.

## ACKNOWLEDGEMENTS

This work was supported by the Carnot ARTS Institute in the framework of RehaByEXO project and the Région Hauts-de-France.

The authors gratefully acknowledge the support of these institutions.

## REFERENCES

- Anderson R., Spong M., 1987, "Hybrid impedance control of robotic manipulators", Proceedings. IEEE International Conference on Robotics and Automation.
- Andrade R. et al., 2019, "Development of a "transparent operation mode" for a lower-limb exoskeleton designed for children with cerebral palsy", 16th International Conference on Rehabilitation Robotics.
- Akdoğan E. et al., 2018, "Hybrid impedance control of a robot manipulator for wrist and forearm rehabilitation: Performance analysis and clinical results", *Mechatronics*, Vol.49, P. 77-91.
- Chen B. et al., 2019, "Knee exoskeletons for gait rehabilitation and human performance augmentation: A state-of-the-art», *Mechanism and machine theory*.
- Denis L. et al., 2016, "Powered robotic exoskeletons in poststroke rehabilitation of gait: a scoping review", *Journal of NeuroEngineering and Rehabilitation* 13:53.
- Esquenazi A. et al., 2017, "Powered Exoskeletons for Walking Assistance in Persons with Central Nervous System Injuries: A Narrative Review", *American academy of physical medicine & rehabilitation*, PM&R 9, P. 46-62.
- Feigin V. et al., 2019, "Global, regional, and national burden of stroke, 1990–2016: a systematic analysis for the Global Burden of Disease Study 2016», *The Lancet Neurology*, Vol. 18, No. 5, P. 439-458.
- Gautier M & al., 2013, "A New Closed-Loop Output Error Method for Parameter Identification of Robot Dynamics », *IEEE Transactions on Control Systems Technology*, Vol. 21, No. 2, P. 428-444.
- Giovacchini F. et al., 2014, "A light-weight active orthosis for hip movement assistance", *Robotics and autonomous system*.
- Manna S. et al., 2018, "Comparative study of actuation systems for portable upper limb exoskeletons", *Medical Engineering & Physics*.
- Olney S. et al., 1996, "Hemiparetic gait following stroke. Part I: Characteristics", *Gait and posture*, Vol. 4, P. 136-148.
- Pennycott A. et al., 2012, "Towards more effective robotic gait training for stroke rehabilitation: a review", *Journal of Neuro Engineering and Rehabilitation*.
- Seo K. et al., 2016, "Fully Autonomous Hip Exoskeleton Saves Metabolic Cost of Walking», *IEEE International Conference on Robotics and Automation (ICRA)*.

Swevers J. & al., 1997, "Optimal robot excitation and identification", IEEE Transactions on Robotics and Automation, Vol. 13, No. 5, P. 730-740.

Tucker M. et al., 2015, "Control strategies for active lower extremity prosthetics and orthotics: a review», Journal of Neuro Engineering and Rehabilitation, 12:1.

